

Stochastic Modelling and Computational Sciences

IMPROVING RAIN FORECASTING ACCURACY THROUGH WAVELET PACKET TRANSFORM IN QUAZIGUND STATION, JAMMU AND KASHMIR, INDIA

Pankaj Sharma¹, Khalil Ahmad², Bilal Rashid^{2,*} and Ambuj Sharma³

¹Department of Mathematics, Ramanujan School of Mathematical Sciences, Pondicherry University, Puducherry, India

²Department. of Mathematics, Al-Falah University, Faridabad, Haryana, India

³Department of Computer Science (AI & ML Branch), NIET, Greater Noida, U.P., India

¹pankajsharma@pondiuni.ac.in, ²kahmad49@gmail.com, ²bilal.mir4@gmail.com and

³ambujsharma1703@gmail.com

*Corresponding Author

ABSTRACT

The study aims to enhance the accuracy of rain predictions by decomposing rainfall data into various frequency components. The investigation involves the utilization of wavelet packet decomposition for feature extraction, allowing for a comprehensive analysis of rain patterns. The proposed approach showcases its potential to improve forecasting models, offering valuable insights for meteorological applications and contributing to more effective water resource management and disaster preparedness. In this paper, we have applied a technique using wavelet packet transform method at pre-processing stage using optimal thresholding technique which convert noisy data into best possible noise-free data, to compare and process the quality data for better forecasting.

Keywords: wavelet packet transform, LSTM, forecasting, deep learning, rain data.

1. INTRODUCTION

In signal processing, considerable emphasis is placed on multiresolution analysis (MRA) and feature extraction. Time-frequency analysis, a robust mathematical approach, is crucial for examining time-varying, non-stationary signals, revealing their joint time and frequency domain distributions. This technique clarifies the intricate relationship between time and signal frequency. Key time-frequency distribution functions include the short-time Fourier transform (STFT), the Gabor transformation, Cohen's class of distributions (e.g., Wigner distribution), enhanced Wigner distribution, Gabor-Wigner distribution, and the S transform. [8].

The strength of the STFT lies in its lucid representation of the energy confined in each frequency element of a signal over a stated time interval, aligning with the intuitive perception of many actual test signals. Despite its widespread use, the STFT grapples with limitations in time or frequency resolution due to the fixed width function of the window, posing challenges in simultaneous optimization [9]. These limitations find resolution through the application of wavelets.

Similar to the Fourier transform, the wavelet transform projects a signal onto a set of basis functions that provide localization in the frequency domain. Unlike the Fourier transform, which offers a uniform time-frequency representation, the wavelet transform excels in offering better high-frequency resolution at low frequencies and improved time resolution at high frequencies. This unique feature stems from the wavelet transform's utilization of a collection of orthogonal bases with varying resolutions, allowing for the precise representation or approximation of a signal through the expansion and translation of the wavelet basis function. This characteristic marks a significant advancement in mathematical analysis compared to the Fourier transform. The versatility of wavelet analysis enables its application across diverse domains, including signal processing, image processing, pattern recognition, and speech analysis.

Wavelet research saw significant advancement in the 1980s. In 1981, Stromberg provided evidence for the existence of wavelet functions, while between 1984 and 1988, Meyer, Battle, and Lemarie developed distinct wavelet basis functions characterized by rapid decay properties [14]. Additionally, Mallat introduced the Mallat

Stochastic Modelling and Computational Sciences

algorithm in 1984, a fast wavelet transform algorithm for signal analysis and reconstruction, based on the concept of Multiresolution Analysis (MRA) [16]. This algorithm, represented by a two-channel filter, enables the approximation of signals, whether in 2-dimensional images or 1-dimensional signals, by a series of sub-signals with varying resolutions. The Mallat algorithm has found extensive use in signal decomposition and reconstruction.

In 1992, Soman and Vaidyanathan introduced wavelet packet theory for designing filter banks [22], which offers a more refined division of the time-frequency plane compared to wavelet transform. This finer division allows for enhanced resolution of the high-frequency segment of the signal, surpassing the capabilities of traditional wavelet analysis.

The forecast rainfall [10, 19] has a broad impact on both agriculture and the travel plan of individuals. However, forecasting rainfall presents a considerable challenge due to its inherent complexity. Various factors, such as humidity, maximum and minimum temperatures, wind speed, and direction, play crucial roles in influencing rainfall patterns [1, 4, 6, 19]. The arrangement of these parameters holds potential for rainfall prediction. Machine-learning algorithms employed for this purpose encompass k-nearest neighbours, decision trees, rule-based methods, and linear regression [7]. Notably, deep learning emerges as particularly effective for larger datasets.

The role of noise in rain forecasting is a subject that has gained increasing attention in meteorological research. Recent studies, such as the work by Sarmad Dashti Latif et al. [19], have underscored the importance of understanding and incorporating noise factors in rain forecasting algorithms. Managing noise in meteorological models and datasets are crucial for improving the accuracy of rain forecasting models. Meteorologists strive to differentiate between relevant signals and random noise to enhance the precision of predictions. Incorporating advanced noise reduction techniques and data filtering methods into forecasting models helps mitigate the impact of irrelevant fluctuations, contributing to more reliable and effective rain forecasting [5, 12, 15]. Recently [1, 10, 11, 13, 19, 23, 24, 25], researchers across the globe are applying wavelet theory with deep learning and machine learning for the prediction (forecasting) of data like wind power, wind energy, traffic prediction, weather, wind speed and rain mass.

This paper aims to utilize the wavelet packet transform (WPT) on the collected rain data with the objective of effectively decomposing the noisy dataset into distinct frequency components. This decomposition enables the isolation and removal of unwanted noise, contributing to a cleaner and more refined dataset. In the context of rain forecasting, where precision is crucial, the reduction of noise in the data through wavelet packet transform facilitates a more robust and effective modeling of rainfall patterns. The application of this transform plays a significant role in improving the signal-to-noise ratio, thereby augmenting the quality of input data and ultimately enhancing the performance of rain forecasting algorithms. We have employed fundamental rainfall parameters including temperature, humidity, and precipitation. Deep learning techniques are utilized to construct the predictive model. Specifically, we propose the implementation of a Long Short-Term Memory (LSTM) model for daily rainfall prediction. Our research focuses on developing a predictive model tailored to the Quazigund district in Kashmir. It is widely recognized that inadequate water supply can have detrimental effects, while excessive water can be either harmful or beneficial depending on various environmental factors, especially in the context of coffee production. Despite existing research on rainfall prediction using techniques such as Artificial Neural Networks (ANN), Multi-layer Perceptron (MLP), and linear regression, there is a dearth of literature on the application of deep learning-based prediction specifically to the Quazigund area.

2. Multiresolution Analysis (MRA) and Wavelets

Understanding MRA is integral to grasping wavelet analysis, as it provides a foundational comprehension of the fundamental concepts underlying wavelets. The space $L^2(P)$ represents the set of square integrable complex-valued functions on P , equipped with the inner product

Stochastic Modelling and Computational Sciences

$$\langle g, f \rangle = \int_{\mathbb{R}} g(x) \overline{f(x)} dx$$

where the bar represents complex conjugation. $l^2(\mathbb{Z})$ is the vector space of square-summable sequences, i.e.

$$l^2(\mathbb{Z}) = \left\{ \{h_k\}_{k \in \mathbb{Z}} : \sum_{k=-\infty}^{\infty} |h_k|^2 < \infty \right\}$$

2.1 Definition [2, 3]. A set of nested closed subspaces $\{V_j\}_{j \in \mathbb{Z}}$ within $L^2(\mathbb{P})$, accompanied by a function $\varphi \in V_0$, is referred to as MRA of the space $L^2(\mathbb{P})$ when this set exhibits following (specific) properties.

- (i) $V_j \subset V_{j+1}, \forall j \in \mathbb{Z}$;
- (ii) $\bigcap_{j \in \mathbb{Z}} V_j = \{0\}$ and $\bigcup_{j \in \mathbb{Z}} V_j$ is dense in $L^2(\mathbb{P})$
- (iii) $f(x) \in V_j$ iff $f(2x) \in V_{j+1}, \forall j \in \mathbb{Z}$;
- (iv) \exists a function $\varphi \in V_0$ such that $\{\varphi(x-k)\}_{k \in \mathbb{Z}}$ forms a Riesz basis (orthonormal basis) for V_0 .
- (v) $f(x) \in V_j \Leftrightarrow f(x-2^{-j}k) \in V_j, \forall k \in \mathbb{Z}$.

The function φ mentioned in (iv) is called a scaling function of the given MRA.

Now, we give the construction of wavelets. Let W_0 be an orthogonal complement of V_0 in V_1 , i.e. $V_1 = V_0 \oplus W_0$. By dilating elements of W_0 by 2^j , we attain a closed subspace W_j of V_{j+1} as

$$V_{j+1} = V_j \oplus W_j, \forall j \in \mathbb{Z}.$$

A function $\psi \in W_0$ whose translates $\{\psi(x-k)\}_{k \in \mathbb{Z}}$ form an orthonormal basis of W_0 is called

a mother wavelet. We make the assumption that such a function is present. Since W_0 and V_0 are subspaces of V_1 , therefore using recursion formula

$$\varphi(x) = \sqrt{2} \sum_k h_k \varphi(2x-k)$$

and
$$\psi(x) = \sqrt{2} \sum_k g_k \psi(2x-k)$$

must exist for some $\{h_k\}, \{g_k\}$ in $l^2(\mathbb{Z})$. We represent the scaled translates of φ and ψ as

$$\varphi_{j,k}(x) = 2^{j/2} \varphi(2^j x - k), \tag{2.1}$$

and
$$\psi_{j,k}(x) = 2^{j/2} \psi(2^j x - k) \tag{2.2}$$

Stochastic Modelling and Computational Sciences

In fact, $\{ \psi_{j,k} : j,k \in \mathbb{Z} \}$ is an orthonormal basis for W_j , $\forall j,k \in \mathbb{Z}$ due to (iv) and by the definition of W_j . Hence $\{ \psi_{j,k} : j,k \in \mathbb{Z} \}$ is an orthonormal basis for $L^2(\mathbb{P})$ [14], which displays that ψ is an orthonormal wavelet on \mathbb{P} .

3. Construction of Wavelet Packets

By generalizing the method of MRA, it is possible to construct wavelet packets. In general, two sequences $\{ \alpha_j \}_{j \in \mathbb{Z}}$ and $\{ \beta_j \}_{j \in \mathbb{Z}}$ in $l^2(\mathbb{Z})$ are considered. Let H be a Hilbert space with orthonormal basis $\{ e_k \}_{k \in \mathbb{Z}}$. Then,

$$f_{2j} = \sqrt{2} \sum_k \alpha_{2j-k} e_k,$$

and

$$f_{2j+1} = \sqrt{2} \sum_k \beta_{2j-k} e_k$$

are orthonormal bases for orthogonal closed subspaces H_1 and H_0 , respectively, such that

$$H = H_1 \oplus H_0$$

By this ‘‘splitting trick’’ [14, 16], we define the basic wavelet packets allied with a scaling function φ as defined in MRA. A graphical representation is shown by Figure 1 (source: MATLAB). The wavelet packets $W_j, j = 0, 1, 2, \dots$ associated with the scaling function φ are defined (recursively) by

$$\omega_{2j}(x) = \sqrt{2} \sum_k h_k \omega_j(2x - k),$$

and

$$\omega_{2j+1}(x) = \sqrt{2} \sum_k g_k \omega_j(2x - k)$$

where $\omega_1 = \psi$ and $\omega_0 = \varphi$ are mother and father wavelets, respectively. Associated with a particular orthonormal scaling function φ , the wavelet packets $\{ \omega_n \}$ defines a family of subspaces of $L^2(\mathbb{P})$ as follows:

$$U_j^n = \text{span} \{ 2^j \omega_n(2^j x - k) \}_{j,k \in \mathbb{Z}}, \quad n = 0, 1, 2, \dots$$

We observe that

$$U_j^0 = V_j, \quad U_j^1 = W_j$$

so that the decomposition into orthogonal components can be expressed as:

$$U_{j+1}^0 = U_j^0 \oplus U_j^1$$

A generalization for alternative values of n may be expressed as:

$$U_{j+1}^n = U_j^{2n} \oplus U_j^{2n+1}, \quad j \in \mathbb{Z}$$

The functions ω_n are obtained by superposition of half scaled translated versions of functions of lower index. But supports of all ω_n are in $[0, 2N-1]$. Therefore, ω_n oscillates approximately n times, and in this context, n can be interpreted as a frequency parameter.

Stochastic Modelling and Computational Sciences

Initial from the ω_n , let us examine the family of wavelet packet atoms characterized by three indices, derived from dyadic dilations and translations of ω_n :

$$\omega_{j,n,k}(x) = 2^{-\frac{j}{2}} \omega_n(2^{-j}x - k)$$

For a given value of j :

$\omega_{j,n,k}(x)$ permit to analyse fluctuations of a given signal around the position $2^j * x$, at the scale 2^j and at various frequencies $\frac{n}{2N}$ for $n=0$ to $2^j - 1$. Some of the refinements of Daubechies wavelet packet with vanishing moment four can be seen in Figure 1 for example.

4. Recurrent Neural Network (RNN):

LSTM stands out as a specialized form of deep learning tool designed to capture long-term dependencies [15]. Unlike traditional neural networks, LSTMs were specifically engineered to overcome challenges associated with retaining information over extended periods. In a deep learning system, the input layer comprises artificial input neurons responsible for delivering pre-processed weather data to subsequent layers for processing [15, 26]. Despite their chain-like structure, LSTMs feature a distinct repeating module consisting of four neural network layers that interact in unique ways. Refer to Figure 2 for an illustration of these modules and their interactions. Employing LSTM, this model leverages five fundamental weather parameters to forecast rainfall based on input parameter values, as depicted in Figure 3.

5. Simulation and Results

The LSTM cell has several components: a cell state, an input gate, a forget gate, an output gate, and a hidden state. Here, h_t is the hidden state; C_t is the cell state; X_t is the input; f_t is the forget gate; o_t is the output gate; i_t is the input gate at time t .

Furthermore, following computations take place at different stages while applying LSTM.

- At Input Gate: $i_t = \sigma(W_i * [h_{t-1}, x_t] + b_i)$
- At Forget Gate: $f_t = \sigma(W_f * [h_{t-1}, x_t] + b_f)$
- At Candidate Cell State: $\bar{c}_t = \tan h(W_c * [h_{t-1}, x_t] + b_c)$
- At Update Cell State: $c_t = f_t * c_{t-1} + i_t * \bar{c}_t$
- At Hidden State: $h_t = o_t * \tan h(c_t)$
- At Output Gate: $o_t = \sigma(W_o * [h_{t-1}, x_t] + b_o)$

Where σ is the sigmoid activation function, $[h_{t-1}, x_t]$ denotes the concatenation of the hidden state and input, W_f, W_i, W_c and W_o are the weight matrices for the corresponding gates and b_f, b_i, b_c and b_o are the bias terms involved in the computational process.

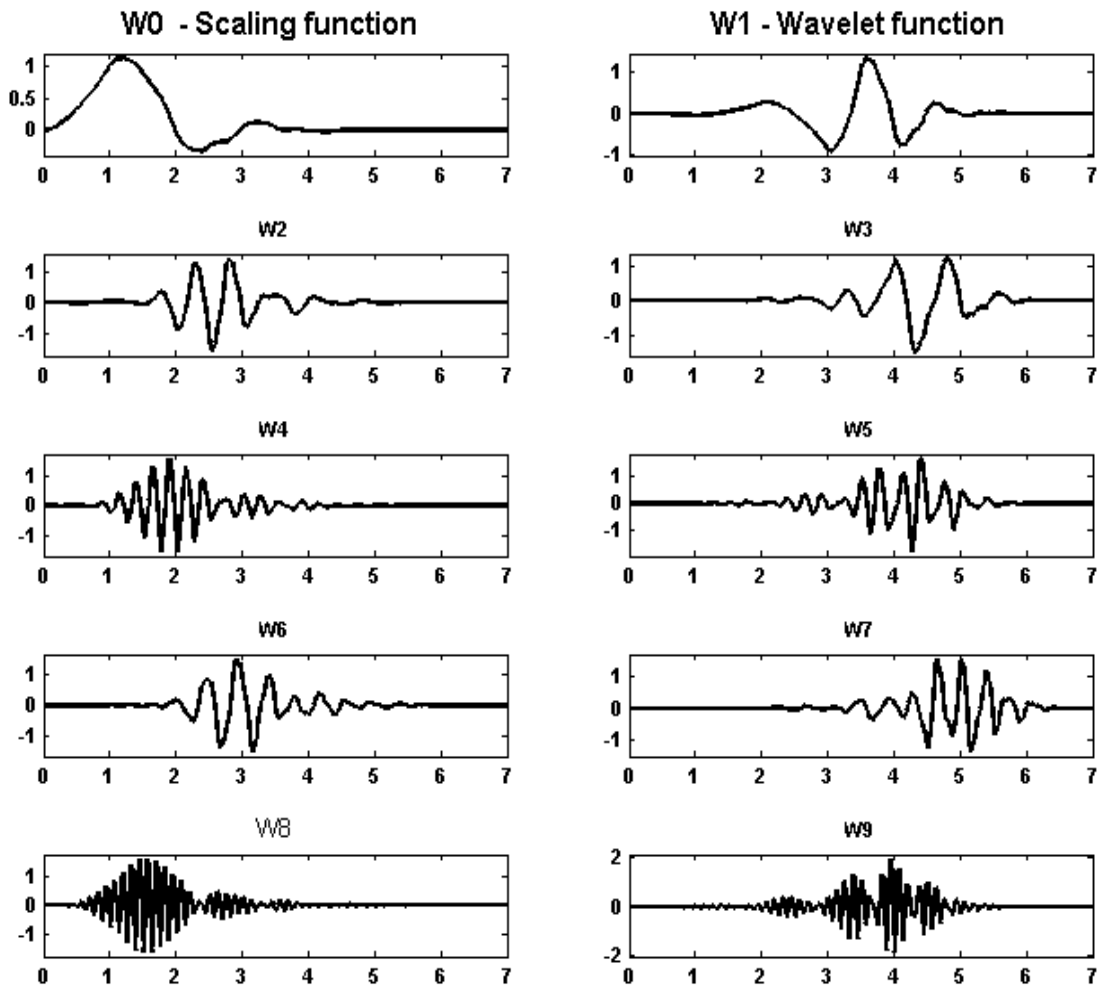


Fig. 1 Wavelet packet (mother wavelet db4) and its refinements

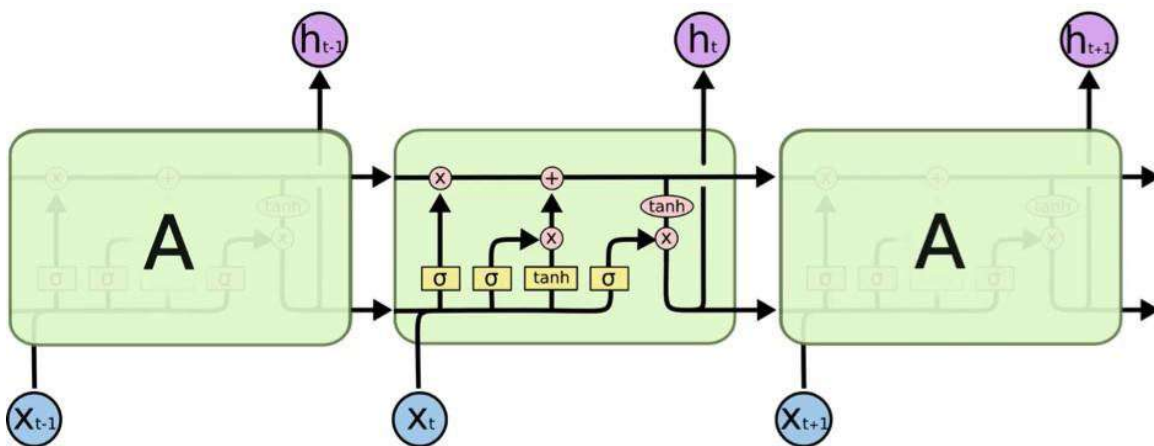


Fig. 2 LSTM Module and Interaction of Components

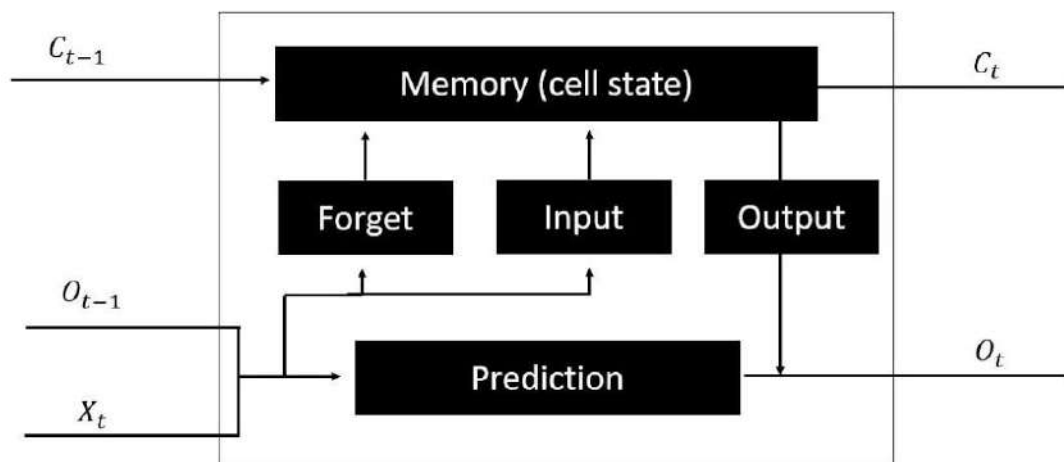


Fig. 3 LSTM Model Cell

5.1 Dataset Description

Considering the duration of the dataset, the continuity of data, and the concurrent observation period, this study utilized a daily weather parameter dataset spanning from 1974 to 2018, comprising 16,435 days of records. The dataset encompasses five parameters, with minimal missing values addressed during preprocessing. To assess stationarity, the Augmented Dickey Fuller Test (ADF Test) was conducted, taking into account the p-value. Weather parameters were derived from the dataset, including the mean of maximum temperature, minimum temperature, morning relative humidity, evening relative humidity, and rainfall. These parameters and their corresponding measurements are mentioned in Table 1. The first five parameters served as inputs, while rainfall was designated as the output variable. The dataset encapsulates a 44-year timeframe, with an 80% train-test ratio utilized for analysis in this study.

Table 1. The Rainfall parameters and their corresponding measurement units

Parameters	Corresponding Measurements
Rain	Millimeter (mm)
Relative Humidity at 8:30	Percentage (%)
Relative Humidity at 17:30	Percentage (%)
Minimum Temperature	Celcius
Maximum Temperature	Clecius

5.2 Data Pre-processing

The data is preprocessed in five stages. In the first four stages (Fig 3.) the dataset underwent cleaning, wherein blank records in the data pertinent to this training were removed. During the preprocessing phase, null values within the dataset were standardized. For precipitation data, missing values were estimated using statistical method in XL STAT 2018. Missing values for daily measured temperature, as well as humidity (relative), were filled using the mean value of the respective data. Initially, missing values were imputed by sampling from a normal distribution with mean and standard error equal to those obtained from available data. Normalization of

Stochastic Modelling and Computational Sciences

weather parameters was performed using a min-max scaler to obtain scaled values, as the feature ranges varied. [17]. The flowchart of such preprocessing data is shown in Figure 4. Finally, we know that white noise is very naturally mixed with the data set while recording. Figure 5, represent the given rain dataset in noisy environments. At final stage we have applied wavelet packet transform to minimise the white noise components from the given dataset. The input layer definition of the LSTM model is often misread. We address this by transforming the data sequence from a two-dimensional matrix to the required three-dimensional format of the input layer, generally known as data reshaping [12].

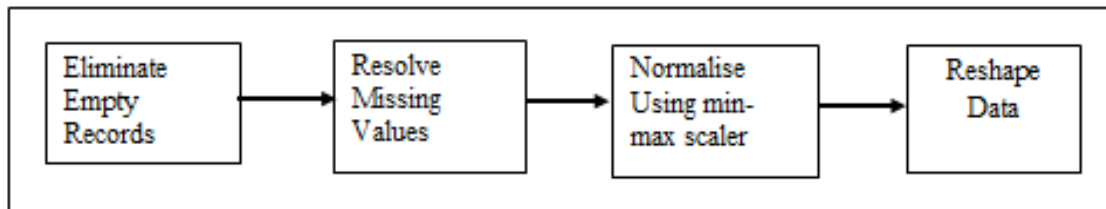


Fig. 4 Data Preprocessing

5.3 Methodology and Discussion

The proposed method is estimated using some fundamental scoring metrics, namely root mean square error (RSME), mean absolute error (MAE) and R^2 -test. The experiment's outcomes are depicted based on LSTM model in wavelet packet transform domain. Furthermore, we assess the prediction accuracy using data obtained from the government of Jammu and Kashmir; India, distinct from the training phase, and evaluate its predictive performance using a testing dataset. The results demonstrate the proposed model's effectiveness in mitigating various types of errors. Figure 4 illustrates the outcomes of the proposed model for estimating rainfall. The results indicate a 98.92% accuracy in forecasting average rainfall (in mm). Consequently, the proposed model holds potential for accurately predicting rainfall on specific days. The plot illustrates the actual daily rainfall values over Quazigund against the predicted rainfall values, with the x -axis representing days and the y -axis representing daily rainfall values.

In this paper, we have proposed a method to investigate the effectiveness of wavelet packet transform for rainfall prediction using historical data which is having some white noise because of the inherent error of the recording machines. Specifically, we have used Haar wavelet as a mother wavelet to extract features from the rainfall time series and then used these features to train a machine learning model for rainfall prediction. We have compared the performance of wavelet analysis using the existing performance metrics techniques.

In this paper, we employ the LSTM and wavelet packet transform algorithms to forecast rainfall. Additionally, various other prediction techniques are employed for the purpose of comparative analysis. One of the metrics is the Mean Squared Error (MSE) quantifies the average squared disparity between the predicted values and the actual values. The formula for calculating the mean squared error is:

$$MSE = \frac{1}{n} \sum_{i=1}^n (y_i - \tilde{y}_i)^2,$$

Where n is the number of data points in the validation set, y_i is the actual value of the i^{th} data point and \tilde{y}_i is the predicted value of the i^{th} data point. Similarly, we have used mean absolute error (MAE) and R^2 - tests to validate the present technique. These examinations are depicted in Table 3.

5.4 Algorithm

- **Collect Rainfall Data:** In this step we have collected rainfall data of Jammu and Kashmir from 1974-2018, which is to be used to train the forecasting model.

Stochastic Modelling and Computational Sciences

(Station: QAZIGUND, District: KULGAM, Division: SRINAGAR, DATE OF INSTALLATION 20-06-1956, HEIGHT A.M.S.L 1690 M, LATITUDE 33 35' N, LONGITUDE 75 05' E)

- **Data Refinement:** We have refined the data e.g. missing values and other kinds of artifacts to make data ready for further processing. We have used 4800 days data from refined dataset. LSTM was employed to analyze fundamental parameters to predict rainfall using them.
- **Perform Wavelet Packet Transform:** It is assumed that the collected rainfall data is corrupted with white noise due to inherent error of the system. We have used wavelet packet transform by using Haar wavelet as a mother wavelet to decompose the signal into different scales. The performance of wavelet packet filter with LSTM can be visualised in Figure 6 for thirty days prediction
- **Feature Extraction:** After performing the previous step, statistical features are extracted from the decomposed signals.
- **Use the Model for Forecasting:** Once the model is validated, it can be used for forecasting rainfall for a future time period based on the weather conditions and other relevant factors. We have used one month data of the year 2018 for model validation.

Table 2: Dataset of Jammu and Kashmir

STNID	Year	Month	Day	TempMax	Temp Min	Rain(mm)	RH 0830	RH 1730
42044	1974	1	1	9.5	-2.7	0.0	96	61
42044	1974	1	2	10.9	-3.6	0.0	96	57
42044	1974	1	3	11.1	-2.6	0.0	93	61
42044	1974	1	4	8.7	-3.2	0.0	93	64
42044	1974	1	5	10.9	-4.1	0.0	88	56
42044	1974	1	6	9.4	-3.1	0.0	96	70
42044	1974	1	7	9.1	-1.3	0.0	89	75
42044	1974	1	8	6.7	-2.0	10.5	97	57
42044	1974	1	9	7.3	-3.0	0.0	93	25
42044	1974	1	10	10.9	-4.1	0.0	85	52
42044	1974	1	11	9.3	-3.2	0.0	90	63
42044	1974	1	12	9.1	-0.3	201.0	100	53
42044	1974	1	13	4.5	-1.7	123.0	100	25
42044	1974	1	14	0.8	-7.0	82.0	100	59
42044	1974	1	15	2.8	-12.1	25.0	100	60
42044	1974	1	16	1.9	-11.4	0.0	100	57
42044	1974	1	17	4.8	-11.3	0.0	x	58
42044	1974	1	18	1.7	-3.6	20.0	89	49
42044	1974	1	19	1.7	-3.6	0.0	95	50
42044	1974	1	20	3.1	-2.9	130.0	100	59
42044	1974	1	21	2.5	-0.9	240.0	100	55
42044	1974	1	22	4.1	-6.4	25.0	92	56
42044	1974	1	23	1.7	-5.4	94.0	93	52
42044	1974	1	24	2.6	-1.3	0.0	93	56
42044	1974	1	25	4.4	-7.5	0.0	92	59
42044	1974	1	26	2.1	-3.3	103.0	100	60
42044	1974	1	27	2.5	-2.3	123.0	93	55
42044	1974	1	28	3.6	-8.5	13.0	x	57

Stochastic Modelling and Computational Sciences

42044	1974	1	29	1.7	-6.7	0.0	x	60
42044	1974	1	30	4.1	-9.2	0.0	x	41
42044	1974	1	31	4.4	-7.5	0.0	82	60

..... *
 * .

STNID	Year	Month	Day	TempMax	Temp Min	Rain(mm)	RH 0830	RH 1730
42044	2017	12	28	11.8	-1.6	0.0	89	64
42044	2017	12	29	12.2	-2.4	0.0	89	69
42044	2017	12	30	12.2	-3.0	0.0	92	66
42044	2017	12	31	10.2	-4.0	0.0	96	67
42044	2018	1	1	10.6	-3.4	0.0	96	74
42044	2018	1	2	10.4	-4.6	0.0	92	62
42044	2018	1	3	10.0	-4.0	0.0	96	61
42044	2018	1	4	9.4	-4.4	0.0	96	58
42044	2018	1	5	9.6	-4.0	0.0	88	68
42044	2018	1	6	8.2	-2.2	0.0	90	60
42044	2018	1	7	8.6	-4.6	0.0	92	58
42044	2018	1	8	9.6	-5.8	0.0	95	58
42044	2018	1	9	10.4	-5.8	0.0	91	57
42044	2018	1	10	10.2	-5.4	0.0	96	50
42044	2018	1	11	9.4	-2.8	0.0	85	58
42044	2018	1	12	12.8	-2.2	0.0	89	52
42044	2018	1	13	12.6	-5.0	0.0	77	49
42044	2018	1	14	13.0	-4.4	0.0	75	48
42044	2018	1	15	13.4	-4.2	0.0	88	48
42044	2018	1	16	12.8	-5.2	0.0	87	52
42044	2018	1	17	9.6	-4.4	0.0	84	70
42044	2018	1	18	11.0	0.4	1.0	90	66
42044	2018	1	19	11.4	-3.0	0.0	93	60
42044	2018	1	20	14.2	-4.0	0.0	45	61
42044	2018	1	21	15.0	-4.2	0.0	85	41
42044	2018	1	22	14.0	-4.4	0.0	85	43
42044	2018	1	23	6.0	-3.2	0.0	85	79
42044	2018	1	24	11.3	-5.2	0.0	85	60
42044	2018	1	25	12.1	-5.0	0.0	88	46
42044	2018	1	26	13.2	-4.2	0.0	88	40

Stochastic Modelling and Computational Sciences

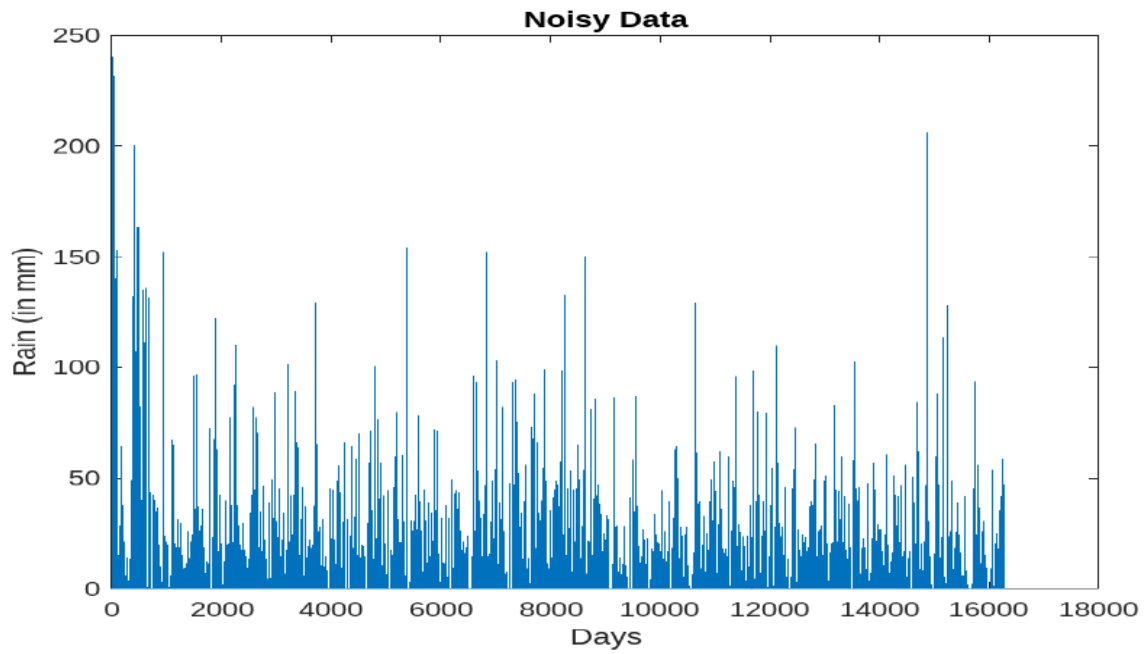


Fig. 5 Noisy Rainfall Data (including missing values)

Table 3. Comparative analysis of different tests with different models

<div style="text-align: center;"> </div>	Decision Tree	SVM	Linear Regression	WPT+LSTM
MSE	0.002714	0.0130270	2.58490	0.001905
MAE	0.008832	0.0312822	1.28178	0.007275
R^2	0.977790	0.9635140	1.00000	0.959836
MSE for the station Banihal	0.002335	0.0312820	1.28178	0.002124
MSE for the station Batotle	0.002321	0.0263510	2.65320	0.002122

Stochastic Modelling and Computational Sciences

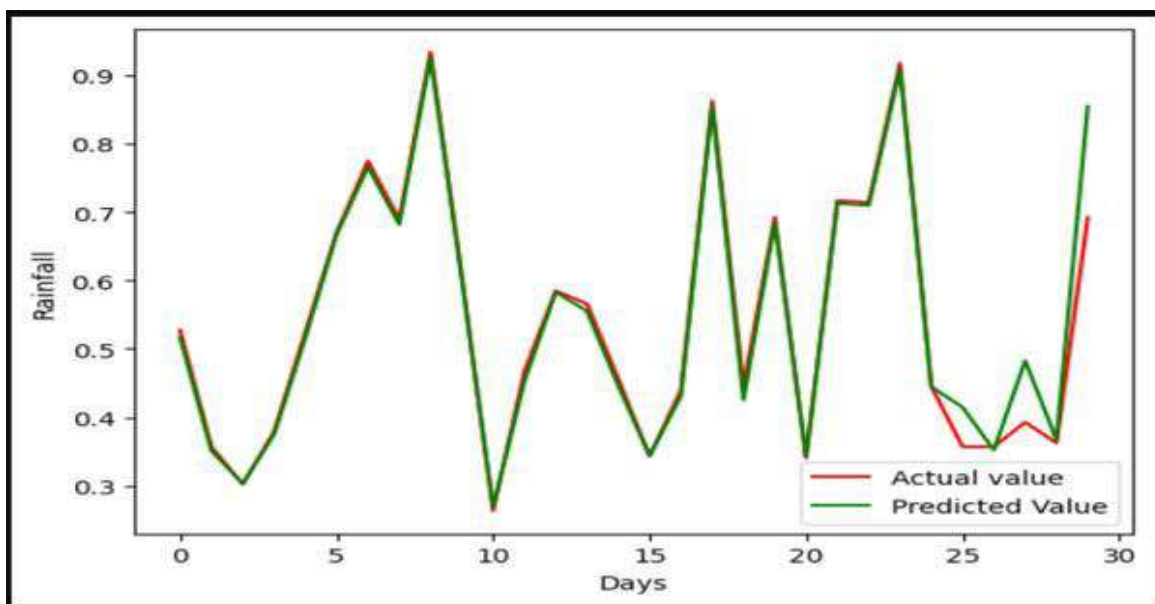


Fig. 6 Forecasting Rainfall for one month using wavelet packet transform

6. CONCLUSION

The investigation into deep-learning techniques for rainfall prediction is outlined, with a focus on developing a rainfall prediction model utilizing LSTM networks and wavelet packet transform for Jammu and Kashmir, India for the data given in Table 2. In general, we have taken three stations viz. Quazigund, Banihal and Batotle and in particular Quazigund station for detail analysis. The dataset comprises daily records of parameters for instance tmax, tmin, relative humidity and rain from 1974 to 2018. Multiple tests and assessments with existing machine learning models are conducted on this dataset to assess and validate the performance of the proposed model. Only 4800 days data has been utilised in the present paper and one month data of the year 2018 has been utilised to validate our proposed model. From Table 3, we observed that in all the testing parameters used in this paper, the LSTM model jointly with wavelet packet transform gives the better performance. As a result, the proposed model is well-suited for various applications where accurate rainfall prediction is essential, including but not limited to smart agriculture. We have used MATLAB and PYTHON for simulation.

An algorithm for rain forecasting using wavelet packet transform has been developed in this paper. This algorithm may be used by meteorologists and weather forecasting agencies to provide accurate and reliable rainfall forecasts, which can help in disaster management and resource allocation. In future, we are planning to create a rainfall prediction model incorporating global wind circulation patterns and climate indices. Additionally, we will try to explore the effects of climate change on rainfall patterns.

Acknowledgements: The authors are thankful to Government of the State Jammu and Kashmir (imd.gov.in) India, for providing Rainfall data.

REFERENCES

- [1] Aasim, S.N. Singh, Abheejeet Mohapatra, Repeated wavelet transform based ARIMA model for very short-term wind speed forecasting, *Renewable Energy*, Volume 136, 2019, Pages 758-768, <https://doi.org/10.1016/j.renene.2019.01.031>.
- [2] Ahmad, K. and Abdullah, 2018. *Wavelet Packets and Their Statistical Applications*. Springer Nature Pte. Ltd., Singapore.

Stochastic Modelling and Computational Sciences

- [3] Ahmad, K. and Shah, F.A., 2013. Introduction to Wavelets with Applications. Real World Education Publishers, New Delhi.
- [4] Ayisha Siddiqua, L. and Senthil Kumar, N. C., 2019. Heavy rainfall prediction using Gini index in decision tree. International Journal of Recent Technology and Engineering (IJRTE), 8 (4), pp. 4558 - 4562.
- [5] Azadi, S., Amiri, H. and Reza Rakhshandehroo, G., 2016. Evaluating the ability of artificial neural network and PCA-M5P models in predicting leachate COD load in landfills. Waste Management, 55, pp. 220-230.
- [6] Carr, M. K. V., 2001. The water relations and irrigation requirements of coffee. Experimental Agriculture, 37 (1), pp. 1-36.
- [7] Chhetri, M., Kumar, S., Roy, P. P. and Kim, B. G., 2020. Deep BLSTM-GRU model for monthly rainfall prediction: a case study of Simtokha, Bhutan. Remote Sensing, 12.
- [8] Cohen, L., 1995. Time-Frequency Analysis. Upper Saddle River, NJ, USA: Prentice-Hall, 5.
- [9] Czerwinski, R. N. and Jones, D. L., 1997. Adaptive short-time Fourier analysis. IEEE Signal Process. Lett., 4(2), pp. 42-45.
- [10] Diao, L., Niu, D., Zang, Z. and Chen, C. 2019. Short-term Weather Forecast Based on Wavelet Denoising and Catboost. Chinese Control Conference (CCC), Guangzhou, China, pp. 3760-3764. doi: 10.23919/ChiCC.2019.8865324.
- [11] Dunne, S. and Ghosh, B. 2013. Weather Adaptive Traffic Prediction Using Neurowavelet Models. IEEE Transactions on Intelligent Transportation Systems, 14(1), pp. 370-379. doi: 10.1109/TITS.2012.2225049.
- [12] Kaur, R., Girdhar, A. and Arora, P., 2017. Detection of rain mass from RADAR images using wavelets. 2nd International Conference on Communication and Electronics Systems (ICES), Coimbatore, India, pp. 424-428. doi: 10.1109/CESYS.2017.8321314.
- [13] Khandelwal, R., Gaurav, K., and Singh, R., 2019. Short-term wind speed forecasting using wavelet transform and support vector regression. Journal of Ambient Intelligence and Humanized Computing, 10(3), pp. 987-999.
- [14] Lei, J., Meyer, Y., and Ryan, R., 1994. Wavelets: Algorithms and applications. Math. Comput., 63, pp. 822.
- [15] Liu, Z., Ding F. and Wan, F., 2021. Wind Speed Forecasting Method Based on Deep Learning Strategy Using Long Short Term Memory Neural Network and Transformer Model. IEEE 23rd Int Conf on High Performance Computing and Communications, pp. 2288-2293. doi:10.1109/HPCC-DSS-SmartCity-DependSys53884.2021.00344.
- [16] Mallat, S. G., 1989. A theory for multiresolution signal decomposition: The wavelet representation. IEEE Trans. Pattern Anal. Mach. Intel., 11(7), pp. 674-693.

Stochastic Modelling and Computational Sciences

- [17] Nasser, A. and Simon, V. 2021. A Novel Method for Analyzing Weather Effect on Smart City Traffic. IEEE 22nd International Symposium on a World of Wireless, Mobile and Multimedia Networks (WoWMoM), Pisa, Italy, pp. 335-340. doi: 10.1109/WoWMoM51794.2021.00061.
- [18] Saiful Bahari, Nurul Iman & Ahmad, Asmala & Burhanuddin, Mohd., 2014. Application of support vector machine for classification of multispectral data. IOP Conference Series: Earth and Environmental Science, 20, 10.1088/1755-1315/20/1/012038.
- [19] Sarmad Dashti Latif et al., 2023. Assessing rainfall prediction models: Exploring the advantages of machine learning and remote sensing approaches. Alexandria Engineering Journal, 82, pp. 16-25. <https://doi.org/10.1016/j.aej.2023.09.060>.
- [20] Soman, A. K. and Vaidyanathan, P. P., 1992. Paraunitary filter banks and wavelet packets. Proc. IEEE Int. Conf. Acoust., Speech, Signal Process. (ICASSP), 4, pp. 397-400.
- [21] Wang, Y. et al., 2021. A review of wind speed and wind power forecasting with deep neural networks, Applied Energy, 304, 117766, <https://doi.org/10.1016/j.apenergy.2021.117766>.
- [22] Wu, S., Jia, L. and Liu, Y. 2021. Ultra-short-term wind energy prediction based on wavelet denoising and multivariate LSTM. Power System and Green Energy Conference (PSGEC), Shanghai, China, pp. 443-447, doi: 10.1109/PSGEC51302.2021.9541909.
- [23] Xiaosheng, P. et al., 2020. Short-Term Wind Power Prediction Based on Wavelet Transform and Convolutional Neural Networks. IEEE/IAS Industrial and Commercial Power System Asia (I&CPS Asia), Weihai, China, pp. 1244-1250. doi: 10.1109/ICPSAsia48933.2020.9208382.
- [24] Yang, P., Zhang, Y., Xia, J. and Sun, S., 2020. Identification of drought events in the major basins of Central Asia based on a combined climatological deviation index from GRACE measurements. Atmos. Res., 244(1), 105105.
- [25] Zhao, Z., Wang, X. L., Zhang, Y. G., Gou, H. Z. and Yang, F. 2017. Wind speed prediction based on wavelet analysis and time series method. International Conference on Wavelet Analysis and Pattern Recognition (ICWAPR), Ningbo, China, pp. 23-27. doi: 10.1109/ICWAPR.2017.8076657.
- [26] Figure 2 and Figure 3 image source: colah.github.io.